

Center of pressure displacement due to graded controlled perturbations to the trunk in standing subjects:
the force-impulse paradigm

Original

Center of pressure displacement due to graded controlled perturbations to the trunk in standing subjects: the force-impulse paradigm / Paterna, Maria; Dvir, Zeevi; De Benedictis, Carlo; Maffiodo, Daniela; Franco, Walter; Ferraresi, Carlo; Roatta, Silvestro. - In: EUROPEAN JOURNAL OF APPLIED PHYSIOLOGY. - ISSN 1439-6319. - ELETTRONICO. - 122:2(2022), pp. 425-435. [10.1007/s00421-021-04844-9]

Availability:

This version is available at: 11583/2952495 since: 2022-01-24T10:20:07Z

Publisher:

Springer

Published

DOI:10.1007/s00421-021-04844-9

Terms of use:

This article is made available under terms and conditions as specified in the corresponding bibliographic description in the repository

Publisher copyright

Springer postprint/Author's Accepted Manuscript

This version of the article has been accepted for publication, after peer review (when applicable) and is subject to Springer Nature's AM terms of use, but is not the Version of Record and does not reflect post-acceptance improvements, or any corrections. The Version of Record is available online at: <http://dx.doi.org/10.1007/s00421-021-04844-9>

(Article begins on next page)

1
2 *Original Article*

3
4 **Center of pressure displacement due to graded controlled**
5 **perturbations to the trunk in standing subjects: the force-**
6 **impulse paradigm**
7
8
9

10 Maria Paterna¹, Zeevi Dvir², Carlo De Benedictis¹, Daniela Maffiodo¹, Walter Franco¹,
11 Carlo Ferraresi¹, Silvestro Roatta^{3*}
12

13
14
15 ¹ Dept. of Mechanical and Aerospace Engineering, Politecnico di Torino, Torino, Italy

16 ² Dept. of Physical Therapy, Faculty of Medicine, Tel Aviv University, Tel Aviv, Israel

17 ³ Dept. of Neuroscience, University of Torino, Torino, Italy
18
19
20
21

22
23
24 *Correspondence to:

25 Silvestro Roatta

26 Dip. di Neuroscienze, Università di Torino

27 c.so Raffaello 30, 10125, Torino, Italy

28 tel +39 011 6708164

29 e-mail: silvestro.roatta@unito.it

30 ORCID: [0000-0001-7370-2271](https://orcid.org/0000-0001-7370-2271)
31
32
33
34
35
36
37
38
39
40
41
42
43
44
45
46
47
48
49
50
51
52
53
54
55
56
57
58
59
60
61
62
63
64
65

1
2
3
4
5
6
7
8
9
10
11
12
13
14
15
16
17
18
19
20
21
22
23
24
25
26
27
28
29
30
31
32
33
34
35
36
37
38
39
40
41
42
43
44
45
46
47
48
49
50
51
52
53
54
55
56
57
58
59
60
61
62
63
64
65

24 **ABSTRACT**

25 *Purpose:* Many studies have investigated postural reactions (PR) to body-delivered
26 perturbations. However, attention has been focused on the descriptive variables of
27 the PR rather than on the characterization of the perturbation. This study aimed to
28 test the hypothesis that the impulse rather than the force magnitude of the
29 perturbation mostly affects the PR in terms of displacement of the center of foot
30 pressure (ΔCoP).

31 *Methods:* Fourteen healthy young adults (7 males and 7 females) received two
32 series of 20 perturbations, delivered to the back in the anterior direction, at mid-
33 scapular level, while standing on a force platform. In one series, the perturbations
34 had the same force magnitude (40 N) but different impulse (range: 2-10 Ns). In the
35 other series the perturbations had the same impulse (5 Ns) but different force
36 magnitude (20-100 N). A simple model of postural control restricted to the sagittal
37 plane was also developed.

38 *Results:* The results showed that ΔCoP and impulse were highly correlated (on
39 average: $r=0.96$) while the correlation ΔCoP -force magnitude was poor ($r=0.48$)
40 and not statistically significant in most subjects. The normalized response,
41 $\Delta\text{CoP}_n=\Delta\text{CoP}/I$, was independent of the perturbation magnitude in a wide range of
42 force amplitude and impulse and exhibited good repeatability across different sets
43 of stimuli (on average: $\text{ICC}=0.88$). These results were confirmed by simulations.

44 *Conclusion:* The present findings support the concept that the magnitude of the
45 applied force alone is a poor descriptor of trunk-delivered perturbations and suggest
46 that the impulse should be considered instead.

1
2
3
4
5
6
7
8
9
10
11
12
13
14
15
16
17
18
19
20
21
22
23
24
25
26
27
28
29
30
31
32
33
34
35
36
37
38
39
40
41
42
43
44
45
46
47
48
49
50
51
52
53
54
55
56
57
58
59
60
61
62
63
64
65

47 **Keywords:** Postural reaction; perturbation; force; impulse; center of pressure; balance
48 control.

49

1
2
3
4
5
6
7
8
9
10
11
12
13
14
15
16
17
18
19
20
21
22
23
24
25
26
27
28
29
30
31
32
33
34
35
36
37
38
39
40
41
42
43
44
45
46
47
48
49
50
51
52
53
54
55
56
57
58
59
60
61
62
63
64
65

50 1. INTRODUCTION

51 Research on postural reactions (PR) has employed a variety of perturbation
52 techniques intended to simulate in laboratory conditions the events that challenge
53 the body equilibrium in real life. Two distinct approaches have been followed:
54 imparting the perturbation i) to the base of support by sliding or tilting the platform
55 (Schmidt et al. 2015; Grassi et al. 2017; Robbins et al. 2017) or ii) directly to the
56 upper body. These two perturbation modes elicit fundamentally different PR
57 (Bortolami et al. 2003; Colebatch et al. 2016; Chen et al. 2017) and thus are both
58 worth to be pursued. However, while the moving platform is easily described and
59 standardized in terms of extent and speed of displacement and rotation, description
60 and quantification of upper body perturbation are more difficult. Direct body
61 perturbation has been achieved in the most disparate of ways. Some devices were
62 based on imparting a pull force to the body by the sudden release of a weight
63 connected to the body via a cable (Martinelli et al. 2015; Maaswinkel et al. 2016;
64 Azzi et al. 2017) or employing electric actuators (Pidcoe and Rogers 1998;
65 Sturnieks et al. 2013; Fujimoto et al. 2015; Robert et al. 2018), which, however,
66 alter the subject's resting posture, thus potentially affecting the overall PR. Others
67 are based on the application of a push force imparted manually by pushing the
68 subject with the hands (Colebatch et al. 2016), or by releasing a pendulum which
69 hits the body at shoulder level (Kim et al. 2012), or by the action of a hand-held
70 device which records the force profile during contact with the subject (Kim et al.
71 2009; Pasman et al. 2019; Dvir et al. 2020). In most cases little attention was
72 devoted to the characterization of the perturbation and the relation between the
73 magnitude of the perturbation and the postural response, focusing instead on the

1
2 74 factors affecting CoP steadiness (Martinelli et al. 2015; Azzi et al. 2017; Grassi et
3
4 75 al. 2017) or its association with the risk of falling (Sturnieks et al. 2013; Fujimoto
5
6 76 et al. 2015). However, the precise identification of the input variable that better
7
8 77 correlates with the CoP response could facilitate the interpretation of the results and
9
10 78 the design of appropriate postural tests. Significantly, it could enhance testing of
11
12 79 patients affected with disorders in which the normal PR may be compromised
13
14 80 (Grassi et al. 2017; Colebatch and Govender 2019).

15
16
17
18
19 81 Although it is generally acknowledged that, within the boundaries of stability, the
20
21 82 greater the magnitude of the perturbation the greater is the PR (Diener et al. 1988;
22
23 83 Kim et al. 2009; Azzi et al. 2017; Forghani et al. 2017; Teixeira et al. 2019), very
24
25 84 few studies investigated this relation with upper body-directed perturbation. Kim et
26
27 85 al (2009) evidenced a positive correlation between the peak force of a body-directed
28
29 86 push perturbation and the displacement of the center of pressure (CoP). However,
30
31 87 by exploring specifically this facet of PR, we have recently observed that in young
32
33 88 men, the magnitude of the CoP response, in terms of its displacement, was better
34
35 89 correlated with the impulse than with the peak force of the postural perturbation
36
37 90 (Dvir et al. 2020). On one hand, it may seem obvious that the magnitude of the
38
39 91 perturbation cannot be simply characterized by the magnitude of the force but
40
41 92 should also depend on the duration of the push. On the other hand, the impulse,
42
43 93 indeed defined as the integral of force over time, has surprisingly not gained much
44
45 94 consideration in the literature, even though it corresponds to the momentum
46
47 95 transferred to the body. As such, it is directly related to the change in speed of the
48
49 96 body and thus to the energy transmitted by the perturbation.
50
51
52
53
54
55
56
57
58
59
60
61
62
63
64
65

1
2 97 The preliminary observation presented in Dvir et al.(2020) did not provide a clear-
3
4 98 cut indication with regard to the impulse vs. force paradigm, possibly because of
5
6
7 99 data dispersion. The postural perturbations were manually delivered, with high
8
9
10 100 intra- and inter- subject variability, in terms of force amplitude, duration and
11
12 101 impulse. This could have accounted for the intra-subject variability of the response
13
14 102 and the low Pearson correlation coefficient values observed in some subjects.
15
16

17 103 Aim of the present study is to reinvestigate the hypothesis that the CoP
18
19 104 displacement due to trunk-directed push perturbations is linearly correlated with the
20
21 105 magnitude of the impulse and not with the force magnitude, by means of a renewed
22
23 106 experimental approach and model simulations. In order to reduce the variability in
24
25 107 the magnitude of the perturbations a novel pneumo-tronic device was developed,
26
27 108 capable of imparting simultaneous force- and duration-controlled perturbations
28
29 109 (Ferraresi et al. 2020a, b; Maffiolo et al. 2020). In addition, the experimental results
30
31 110 are discussed and compared with a simulation of the CoP response based on a
32
33 111 simple single-link inverted pendulum model.
34
35
36
37
38
39
40

41 112 **2. METHODS**

42 113 *2.1 Experimental test*

43 114 2.1.1 Subjects

44 115 A group of 14 healthy young adults, 7 females (mean(SD) age: 22.7(1.7)years;
45
46 116 height: 1.62(0.05)m; weight: 54.0(4.2)kg; BMI: 20.7(1.5)kg/m²) and 7 males
47
48 117 (mean(SD) age: 23.1(2.7)years; height: 1.78(0.11)m; weight: 70.3(6.0)kg; BMI:
49
50 118 22.3(1.6)kg/m²), was recruited from the student population at the Politecnico di
51
52
53 119 Torino. Exclusion criteria included: recent lower extremity injury and/or fracture
54
55
56
57
58
59
60
61
62
63
64
65

1
2 120 (< 1 year), previous reconstructive surgery in the lower extremity and balance
3
4 121 deficits. All subjects provided written informed consent to participate in this study
5
6 122 which was approved by the institutional review board of the University of Torino
7
8
9 123 (Prot. n. 380583).
10

11 12 13 14 124 2.1.2 Task and instrumentation

15
16 125 The experimental task consisted of recovering balance following impulsive
17
18 126 perturbations applied to the trunk in the anterior direction while standing on a force
19
20
21 127 platform.
22

23
24 128 The force platform, a modified Shekel (Beit Keshet, Israel) device, was made up of
25
26 129 a still plate (52x36 cm) which was supported by 4 uniaxial load cells (TEDEA,
27
28 130 Israel, model 1042, rated capacity 100 kgf), mounted on a base plate. The
29
30
31 131 perturbation was applied by a pneumo-tronic perturbator designed and constructed
32
33
34 132 at the Dept. of Mechanical and Aerospace Engineering at the Politecnico di Torino.
35
36 133 The instrument is shown in Fig. 1A and was described in detail in another
37
38 134 publication (Ferraresi et al. 2020b). The closed-loop force feedback design, based
39
40
41 135 on the continuous monitoring of the perturbation force provided by a load cell
42
43 136 positioned in series with the tip of the perturbator, allows for the regulation of the
44
45
46 137 precise intensity and duration of the stimulus delivered to the subject, irrespective
47
48
49 138 of the mechanical compliance of the operator (Ferraresi et al. 2020b).
50

51 52 53 139 2.1.3 Procedure

54
55 140 During the test, the subjects stood barefoot on the force platform with the feet at
56
57
58 141 pelvic distance and with vision unobstructed. Subjects were asked to assume a
59
60
61
62
63
64
65

1
2 142 normal-relaxed stance and they were instructed to respond naturally. The feet
3
4 143 locations were traced onto the platform surface to ensure consistent initial foot
5
6
7 144 placement across test sessions for each participant. The operator stood behind the
8
9 145 subject holding the perturbator while the interface was maintained at a distance of
10
11
12 146 about 2 cm from the subject's back (Fig. 1B). Immediately before the starting of
13
14 147 the test, participants were familiarized with the procedure by receiving few
15
16 148 perturbations. The perturbations were delivered to the trunk always at inter-scapular
17
18 149 level (IS), given that, at this site, more reproducible responses could be obtained,
19
20 150 compared to lumbar level (Dvir et al. 2020).
21
22
23

24
25 151 The test comprised two series, with a break of 5 min in between. In one series,
26
27 152 namely the constant-force series, the perturbations had the same force magnitude
28
29 153 (40 N), but different impulse values (2 Ns; 4 Ns; 6 Ns; 10 Ns). In the other series,
30
31 154 namely the constant-impulse series, the perturbations had the same impulse (5 Ns)
32
33 155 but different force magnitude (20 N; 40 N; 60 N; 100 N). Based on our previous
34
35 156 experience, we operated in a range of values large enough to elicit a clearly
36
37 157 detectable response and small enough to exclude a step response. The values of 40
38
39 158 N and 5 Ns were arbitrarily chosen as intermediate values within that range. The
40
41 159 average force perturbation profiles, for each condition, are shown in Fig. 2.
42
43
44
45
46

47 160 In each series, the subjects received a total of 20 perturbations, 5 for each force
48
49 161 profile mentioned above. The sequences of perturbations, each one including 5
50
51 162 equal stimuli, were provided in random order. An inter-perturbation pause of at
52
53 163 least 10 s was allowed for returning to relaxed stance. The order of the 2 series was
54
55 164 randomized as well. A typical testing session lasted about 20 minutes.
56
57
58
59
60
61
62
63
64
65

1
2 165 2.1.4 Data processing
3

4 166 Data were extracted and processed with custom routines developed in
5
6 167 MATLAB_R2019b®. The force signal was acquired at 1000 Hz and digitally low-
7
8
9 168 pass filtered using a dual-pass 8th order Butterworth filter with a cut-off frequency
10
11 169 of 200 Hz. The actual magnitude of the perturbation was characterized in terms of:

- 12
13
14
15 170 • Force Amplitude (in N): the average force at the plateau. The start and the
16
17 171 end of the plateau were automatically detected as the time instants at which
18
19 172 the force signal crossed a threshold equal to 95% of the intended force
20
21 173 magnitude (see Fig. 3).
22
23
24 174 • Impulse (in Ns): the integral of force computed over the time interval in
25
26 175 which the force is greater than 0.5 N.
27
28
29

30 176 The ground reaction forces were acquired at 1000 Hz and were used to calculate
31
32 177 the coordinates of the CoP. Both coordinates were digitally low-pass filtered with
33
34 178 a dual-pass 8th order Butterworth filter with a cut-off frequency of 20 Hz. The
35
36 179 postural response, ΔCoP , was computed as the maximum CoP displacement,
37
38 180 observed within 2 s from the perturbation. The displacement (in cm) is calculated
39
40 181 from the average resting position, calculated over the 3 s preceding the perturbation.
41
42
43
44
45
46

47 182 2.1.5 Statistical Analysis
48

49 183 All statistical procedures were conducted using MATLAB_R2019b®.
50

51
52 184 Possible differences in impulse and force amplitude among the different
53
54 185 perturbation types were analyzed through a Friedman test with grouping factor
55
56
57
58
59
60
61
62
63
64
65

1
2 186 impulse and force amplitude for the constant-force and constant-impulse series,
3
4 187 respectively.

5
6
7 188 Pearson's correlation coefficient (r) was used to assess the relationship between
8
9 189 Δ CoP and the perturbation. The Fisher's Z transform was used to estimate an
10
11 190 average correlation coefficient over all subjects. Pearson's coefficient was also
12
13 191 calculated to evaluate the relationship between the postural response and the
14
15 192 physical characteristics of the subjects. The Friedman's test was used to determine
16
17 193 whether the impulse or force amplitude affect the CoP displacement.

18
19
20 194 Intraclass correlation coefficients ($ICC_{3,k}$), based on a mean rating ($k = 5$), absolute
21
22 195 agreement, 2-ways mixed effects model were derived to quantify the reliability of
23
24 196 the CoP response among different stimulus magnitudes while the coefficient of
25
26 197 variation (CoV) was used to assess the variability of the responses to the same
27
28 198 perturbation type. In order to evaluate whether general postural adjustments in
29
30 199 anticipation of back perturbations took place during the test, changes in resting CoP
31
32 200 were assessed within each session (comparing the beginning and the end of each
33
34 201 experimental session, average CoP computed 30-s intervals with no perturbations;
35
36 202 Wilcoxon Signed Rank Test) as well as within each of the 8 sequences of stimuli
37
38 203 of the same type (comparing the 3-s CoP baseline preceding the first stimulus and
39
40 204 the last one of the sequence; Wilcoxon Signed Rank Tests, with Bonferroni
41
42 205 correction).

43
44
45 206 Data in the text are expressed as mean \pm standard deviation.

46
47
48 207 *2.2 Single-link inverted pendulum models*

1
2 208 The human body orthostatic position perturbed with low entity disturbances
3
4 209 occurring in the sagittal plane can be schematized by means of an inverse pendulum
5
6 210 model (Winter et al. 1998). The basic scheme, implemented in MATLAB®
7
8 211 Simulink® environment, represents the body as a rigid link having a single
9
10 212 rotational degree of freedom (DoF) about the ankle joint (Fig. 4). For small
11
12 213 oscillations of the body θ , the linearization of the model yields the following
13
14 214 equations:

15
16
17
18
19
20
21 215
$$\tau + mgd\theta - md^2 \frac{d^2\theta}{dt^2} - I \frac{d^2\theta}{dt^2} + F_e h_F = 0 \quad (1)$$

22
23 216
$$CoP = \frac{-\tau - R_x h}{mg} \quad (2)$$

24
25
26 217 where τ is the correcting torque at the ankle, m is the body mass, g is the
27
28 218 gravitational acceleration, d is the distance between ankle joint and the center of
29
30 219 mass (CoM), I is the rotational inertia of the body about the CoM, h_F is the distance
31
32 220 between ankle joint and the point of application of the perturbation force F_e , CoP is
33
34 221 the center of pressure position, R_x is the horizontal component of the ground
35
36 222 reaction force, h is the height of ankle joint with respect to the fixed base of support.

37
38
39 223 Although simplified models of balance control can focus on muscle stiffness alone
40
41 224 as the main tool to achieve stabilization in quiet standing, it is well known that such
42
43 225 passive behavior is generally not sufficient to ensure stability (Morasso et al. 1999),
44
45 226 especially when significant external disturbances are considered. For this reason,
46
47 227 the correcting torque at the ankle τ has been modeled as the sum of a passive and
48
49 228 an active contribution. The passive contribution is related to the visco-elastic
50
51 229 behavior of human tissues and is proportional to both the deformation θ and the rate
52
53
54
55
56
57
58
59
60
61
62
63
64
65

1
2 230 of deformation $\dot{\theta}$ of the joint (Engelhart et al. 2015), whereas the active contribution
3
4
5 231 depends on the neuromuscular control managed by the central nervous system and
6
7 232 can be modeled as a delayed PD (Proportional-Derivative) action (Van Der Kooij
8
9 233 et al. 2005). In particular, the output of the controller, i.e., the active torque at the
10
11
12 234 ankle, is aimed at minimizing the error θ , i.e., the current angular displacement from
13
14
15 235 the initial standing position ($\theta=0$). The information about the current angular
16
17 236 displacement is fed to the controller by noisy and delayed sensory feedback. Thus,
18
19 237 a constant transmission delay was introduced as the latency between the variation
20
21
22 238 of θ and the generation of the reflex active torque (Goodworth and Peterka 2018),
23
24 239 and an additive pink noise was introduced to account for the limitations of the
25
26
27 240 sensory system (Van Der Kooij and Peterka 2011; Boonstra et al. 2013; Goodworth
28
29 241 and Peterka 2018). Proportional and derivative gains of the PD control model then
30
31
32 242 need to be identified, to match the characteristics of a given subject and to achieve
33
34 243 stability. (Van Der Kooij et al. 2005; Van Der Kooij and Peterka 2011; Goodworth
35
36 244 and Peterka 2018).

37
38
39
40 245 With the limited aim of investigating the theoretical dependence of the CoP
41
42 246 response to force and impulse of the perturbation, the model was configured as
43
44
45 247 follows: 1) anthropometric parameters were set equal to average values computed
46
47 248 over the participants to the experimental study (with reference to Fig. 4: $m = 62$ kg,
49
50 249 $l = 1.70$ m, $h = 0.1$ m, $d = 0.6l$, $I = ml^2/12$, $h_F = 1.2$ m); 2) the coefficients of the
51
52 250 passive response were set according to the literature (Engelhart et al. 2015); 3) the
53
54 251 latency between the generation of the active torque and the variation of θ was set to
55
56
57 252 the constant value of 90 ms, according to the literature (Goodworth and Peterka
58
59
60
61
62
63
64
65

1
2 253 2018); 4) active control parameters and noise level were estimated by an iterative
3
4 254 least-squares fitting used to match the simulation with the average experimental
5
6
7 255 postural response.
8
9

10 256 The CoP response to a given perturbation was obtained from the average of 5
11
12 257 distinct simulations, thus accounting for the variability introduced by sensory noise.
13
14
15

16 17 258 **3. RESULTS**

18 19 259 *3.1 Results of the experimental trials*

20
21 260 A representative recording of a single perturbation along with the postural response
22
23 261 is shown in Fig. 3.
24
25

26
27 262 The actual magnitudes for the different experimental perturbation types are shown
28
29 263 in Fig. 5 for the two series. In the constant-force series, the perturbator delivered
30
31 264 stimuli with different impulses and with similar force amplitude values (on average,
32
33 265 39.54 ± 3.01 N) although the actual force amplitude appeared to depend on stimulus
34
35 266 type ($p < 0.01$) (Figure 5A). Similarly, the perturbation types in the constant-
36
37 267 impulse series were well characterized by distinct force values and similar impulse
38
39 268 values (on average, the impulse was equal to 4.60 ± 0.28 Ns) although a significant
40
41 269 dependence of impulse on stimulus type was observed ($p < 0.01$) (Fig. 5B).
42
43
44
45

46
47 270 Note that, while impulse was precisely controlled among subjects, peak force
48
49 271 exhibited some increased dispersion at 2 Ns compared to other impulse levels,
50
51 272 possibly due to the difficulty in controlling short-duration perturbations.
52
53
54
55
56
57
58
59
60
61
62
63
64
65

1
2 273 In all subjects, ΔCoP exhibited a significant ($p < 0.001$) and extremely good linear
3
4 274 correlation with the impulse of the perturbation (Fig. 6A), $r = 0.96$ on average, in
5
6
7 275 spite of the slight differences observed in average peak force levels. Conversely,
8
9 276 the mean correlation between ΔCoP and force amplitude was poor ($r = 0.49$) and
10
11 277 not statistically significant in 7 out of 14 subjects (Fig. 6B). The box plots of Fig.
12
13 278 6C show the distribution of the individual Pearson's correlation coefficients in the
14
15
16
17 279 two cases.

18
19
20 280 The linearity of the relation between ΔCoP and impulse allowed normalizing the
21
22 281 CoP displacement to the impulse of the perturbation: $\Delta\text{CoP}_n = \frac{\Delta\text{CoP}}{\text{Impulse}}$, which
23
24
25 282 should then provide a postural index independent of the magnitude of perturbation
26
27 283 (Dvir et al. 2020). This index remained fairly constant, within the constant-force
28
29 284 series for impulse (range: 4-10 Ns). Friedman's ANOVA indicated a significant
30
31 285 dependence of ΔCoP_n with impulse ($p < 0.01$) with a significantly increased value
32
33 286 at impulse = 2 Ns compared to the other magnitudes ($p < 0.01$) (Fig. 7A). Also in
34
35 287 the constant-impulse session, the experimental ΔCoP_n was influenced by the force
36
37 288 amplitude of the perturbation ($p < 0.01$) but only the response to $F=100$ N differed
38
39 289 significantly from the other magnitudes (Fig. 7B): the ΔCoP_n at 100 N was
40
41 290 significantly higher than the ΔCoP_n at 20 N ($p < 0.05$) and at 40 N ($p < 0.01$).
42
43 291 Notably, on exclusion of the low-impulse (2 Ns) and high-force perturbations (100
44
45 292 N) the individual ΔCoP_n values remain fairly comparable, even in response to
46
47 293 different stimulus types (ICC = 0.88 with 95% confident interval [0.75 – 0.96]).
48
49 294 Furthermore, the normalized index ΔCoP_n showed relatively low variability when
50
51 295 assessed in response to 5 perturbations of the same type: on average $\text{CoV} = 13 \pm 7\%$.
52
53
54
55
56
57
58
59
60
61
62
63
64
65

1
2 296 A single index value was calculated for each subject by averaging the ΔCoP_n over
3
4 297 all perturbations greater than 2 Ns and less than 100 N (mean [range]: 0.93 [0.72 –
5
6
7 298 1.15] cm/Ns). The mean value of the ΔCoP_n was significantly inversely correlated
8
9 299 with the physical characteristics of the subjects: weight ($r = -0.79$), height ($r = -$
10
11 300 0.69) and foot length ($r = -0.63$).

12
13
14
15 301 In order to exclude postural adjustments in preparation for back perturbations, the
16
17 302 resting CoP was analyzed for possible variations during the test. No significant
18
19 303 change in resting CoP was detected within any of the 2 session and of the 8
20
21 304 perturbation sequences.

22 23 24 25 26 305 *3.2 Simulations results*

27
28 306 The tuning of the model was performed to match the average experimental ΔCoP_n
29
30 307 response of Fig. 7A (black line). The comparison between simulation results and
31
32 308 experimental data, for each testing condition selected during the trials carried out
33
34 309 on healthy subjects, is shown in Fig. 8.

35
36 310 It can be observed that, in the absence of sensory noise, simulated ΔCoP exhibited
37
38 311 a linear trend with the impulse (Fig. 8A, blue line) whereas no dependence on the
39
40 312 force amplitude (Fig. 8B) was found. Accordingly, ΔCoP_n remained extremely
41
42 313 constant over the entire range of impulse and force amplitude (Fig. 8C and D).

43
44 314 With the addition of noise to the sensory feedback, both ΔCoP and ΔCoP_n increased
45
46 315 in all conditions (Fig 8 A-D, red lines). While this effect was uniform for ΔCoP in
47
48 316 all conditions, it was particularly marked at low impulse for ΔCoP_n , thus faithfully
49
50 317 matching the experimental data at 2 Ns.

1
2 318 **4. DISCUSSION**

3
4 319 To the best of our knowledge, this is the first study in which force and impulse of
5
6 320 the trunk perturbations have been systematically varied in order to investigate their
7
8
9 321 differential effect on PR. The issue was addressed by challenging the balance of
10
11 322 healthy subjects by means of a custom-built perturbator, which proved adequate to
12
13 323 deliver accurately controlled stimuli, and by analyzing simulated responses based
14
15
16 324 on a simple inverse pendulum model.

17
18
19 325 The findings support the hypothesis formulated on the basis of a previous
20
21 326 observation, namely, that the displacement of the CoP is consistently and strongly
22
23 327 correlated with impulse and not significantly correlated with the force amplitude of
24
25
26 328 the perturbation. Furthermore, since the extracted ΔCoP_n was quite constant across
27
28
29 329 the perturbation range, the applicability of this index as a synthetic descriptor of the
30
31 330 individual postural performance was further amplified.

32
33
34
35 331 Although, as pointed out, the association between ΔCoP and the magnitude of the
36
37 332 perturbation has been highlighted before, a clear *linear* relationship has been
38
39 333 evidenced experimentally only in a handful of studies. Kim et al (2009) showed that
40
41
42 334 ΔCoP was positively correlated with the peak force of perturbations applied to the
43
44 335 high back, in apparent contrast with the present results. However, we speculate that
45
46
47 336 the duration of the perturbations (which was not measured) was quite constant
48
49 337 across the different subjects, which would make impulse and force amplitude
50
51
52 338 proportionally related and thus, both correlated with ΔCoP . Our preliminary study
53
54 339 on PR (Dvir et al. 2020) indicated a moderate correlation between ΔCoP and force
55
56
57 340 ($r = 0.50$) and a stronger correlation with the impulse of the perturbation ($r = 0.71$)

1
2 341 but the distributions of the individual Pearson correlation coefficients were quite
3
4 342 dispersed, possibly because the study was based on uncontrolled manually-
5
6 343 delivered perturbations. The possibility to deliver accurate perturbations in the
7
8 344 present study effectively reduced the intra-subject variability in the PR and revealed
9
10 345 the clear-cut linear relationship between ΔCoP and impulse ($r = 0.96$) while
11
12 346 confirming a low correlation between ΔCoP and force amplitude ($r = 0.49$ on
13
14 347 average but reaching significance only in 7 subjects). Moreover, the reproducibility
15
16 348 of the disturbances provided by the perturbator was adequate for the application, as
17
18 349 signaled by the results shown in Fig. 5, confirming that the performance of the
19
20 350 device was not significantly affected by the presence of a human operator (Ferraesi
21
22 351 et al. 2020b; Maffiodo et al. 2020). Notably, as compared to our previous study
23
24 352 based on manual uncontrolled perturbations, with the new perturbator we were able
25
26 353 to reduce the within-subject variability of ΔCoP_n , from about $20 \pm 8\%$ (recalculated
27
28 354 from previous data) to $13 \pm 7\%$. As a result, it was here possible to achieve a
29
30 355 comparable ICC with as few as 5 perturbations, instead of the 20 stimuli used in the
31
32 356 previous study.

33
34 357 The results of the study reinforce the concept that a single index, ΔCoP_n , obtained
35
36 358 from the ratio of ΔCoP and impulse, may synthetically describe the PR of the
37
38 359 subject, independently of the magnitude of the perturbation (Dvir et al. 2020). In
39
40 360 fact, this index is here shown to remain fairly constant in a wide range of force and
41
42 361 impulse intensity (Fig. 7). Notably, this index was slightly but significantly
43
44 362 increased at low impulse and high force amplitude: a pattern not predicted by the
45
46 363 model (Fig. 8 D). While significant non-linearities are embedded in the postural
47
48 364 control system, starting from the muscle level (Ivanenko and Gurfinkel 2018), the
49
50
51
52
53
54
55
56
57
58
59
60
61
62
63
64
65

1
2 365 present deviation from linearity could be related to the short duration of the
3
4 366 perturbation, which is below 75 ms for both 2 Ns and 100 N. In fact it has been
5
6
7 367 proposed that short stimuli elicit a triggered response, uninfluenced by the stimulus
8
9 368 characteristics, while a longer stimulus duration would be necessary for sensory
10
11 369 inputs to encode the magnitude of the perturbation and help to shape a proportionate
12
13 370 response (Diener et al. 1988). On the other hand, the results here obtained with the
14
15 371 model also suggest that, at low perturbation magnitudes, the presence of noise in
16
17 372 the system may account for a similar non-linearity (Fig 8 C-D).
18
19
20
21
22

23 373 While the implemented model completely excludes a dependence of the PR on the
24
25 374 force amplitude, a significant correlation was evidenced in some subjects (Fig. 6B).
26
27 375 It may be observed that these individual correlations are based on only 4 points and
28
29 376 thus heavily depend on each single measurement. As a consequence, increased
30
31 377 correlations would result due to the abnormally increased response at 100 N, as
32
33 378 previously discussed. On the other hand, a weak correlation with the force
34
35 379 amplitude could also result from the involvement of additional sensory feedback
36
37 380 pathways, particularly sensitive to the force stimulus (e.g., touch receptors of the
38
39 381 back, vestibular receptors), not included in the present model.
40
41
42
43
44
45

46 382 Regarding the accuracy of the simulations, the approach to model tuning used in
47
48 383 this study was considered suitable to achieve a realistic although simplified
49
50 384 behavior of the model, however it is well known that all the active and passive
51
52 385 response parameters discussed are highly subject-specific and require accurate
53
54 386 estimation when a detailed description of balance control is targeted (Goodworth
55
56 387 and Peterka 2018).
57
58
59
60
61
62
63
64
65

1
2 **388 5. LIMITATIONS**
3
4

5 389 As a first approximation, the balance reaction of healthy young adults in response
6
7 390 to low disturbance mainly consists of a correcting torque at the ankle (Horak and
8
9 391 Nashner 1986; Shumway-Cook and Woollacott 2007). Therefore, a single-link
10
11 392 inverted pendulum model was developed to simulate the postural response of the
12
13 393 study participants. This approximation was supported by the visual inspection of
14
15 394 the experimental trials, that confirmed how most oscillations occurred about the
16
17 395 ankle joints. As indicated by the good match between experimental and simulated
18
19 396 data, this simple model proved to be sufficiently accurate for the purpose of testing
20
21 397 the relationship between the displacement of the CoP and the impulse of the
22
23 398 perturbation. On the other hand, we cannot exclude that other postural strategies,
24
25 399 such as the hip strategy, could also contribute to the whole response, particularly to
26
27 400 high-magnitude perturbations. This would likely affect the correlation between
28
29 401 ΔCoP_n and impulse, although the precise effects are difficult to predict, based on
30
31 402 the present experiments. Appropriate integration of the hip strategy into the model
32
33 403 requires to adopt a double-link inverted pendulum model, resulting in a far more
34
35 404 complex optimization problem, with additional unknown control parameters used
36
37 405 to model the correcting torque at the hip and the interaction between active controls
38
39 406 at each joint (Goodworth and Peterka 2018). This, in turn, requires the acquisition
40
41 407 of additional descriptors of the postural response, e.g. tangential forces at the
42
43 408 platform, movements and acceleration of the different body segments. The present
44
45 409 results suggest that this increase in complexity is not necessary for describing the
46
47 410 response to small postural perturbation.
48
49
50
51
52
53
54
55
56
57
58
59
60
61
62
63
64
65

1
2 411 Another limitation of the study was the non-exactly constant value of the force
3
4 412 amplitude and of the impulse in the force constant session and in the impulse
5
6 413 constant session, respectively. The perturbations were applied to the subjects with
7
8 414 a custom-made device consisting of a low friction pneumatic actuator controlled in
9
10 415 force and position by a PI controller. The nonlinearities and relatively slow
11
12 416 dynamics associated to pneumatic systems and the inertia of the piston make the PI
13
14 417 controller not able to appropriately minimize the error between the force reference
15
16 418 profile and the applied force in a very short time. As a result, there is an overshoot
17
18 419 in the first 35 ms of the perturbation that impacts on the calculated Force Amplitude,
19
20 420 especially in the case of short-lasting perturbations. To obtain more accurate
21
22 421 perturbation profiles and more robust control, an electrically-actuated perturbator
23
24 422 based on Model Predictive Control, with inherent high dynamics and stiffness, is
25
26 423 currently under development (Pacheco Quiñones et al. 2021).
27
28
29
30
31
32
33
34
35

36 424 **6. CONCLUSION**

37
38
39 425 The results support the use of the impulse rather than the force as input variable in
40
41 426 impulsive perturbations applied to the trunk. Thanks to the linearity of the
42
43 427 relationship between ΔCoP and impulse, the postural index, ΔCoP_n , may be used
44
45 428 as a synthetic descriptor of the individual postural performance.
46
47
48
49
50

51 429 **CONFLICT OF INTEREST STATEMENT**

52
53
54 430 The authors have no conflict to disclose.
55
56
57

58 431 **ACKNOWLEDGMENTS**

1
2
3
4
5
6
7
8
9
10
11
12
13
14
15
16
17
18
19
20
21
22
23
24
25
26
27
28
29
30
31
32
33
34
35
36
37
38
39
40
41
42
43
44
45
46
47
48
49
50
51
52
53
54
55
56
57
58
59
60
61
62
63
64
65

432 This work was supported by grants from “Fondo Europeo di sviluppo regionale –
433 Regione Liguria” (ROAS_RIC_COMP_17_01) and by “Proof of Concept” Project
434 2018, the Politecnico di Torino. Funding sources had no role in the conduction of
435 the study.

1
2 436 **REFERENCES**
3
4

- 5
6 437 Azzi NM, Coelho DB, Teixeira LA (2017) Automatic postural responses are
7
8 438 generated according to feet orientation and perturbation magnitude. *Gait*
9
10 439 *Posture* 57:172–176. doi: 10.1016/j.gaitpost.2017.06.003
11
12
13
14 440 Boonstra TA, Schouten AC, Van Der Kooij H (2013) Identification of the
15
16 441 contribution of the ankle and hip joints to multi-segmental balance control. *J*
17
18 442 *Neuroeng Rehabil* 10:23. doi: 10.1109/TNSRE.2014.2372172
19
20
21
22 443 Bortolami SB, DiZio P, Rabin E, Lackner JR (2003) Analysis of human postural
23
24 444 responses to recoverable falls. *Exp Brain Res* 151:387–404. doi:
25
26 445 10.1007/s00221-003-1481-x
27
28
29
30
31 446 Chen B, Lee YJ, Aruin AS (2017) Role of point of application of perturbation in
32
33 447 control of vertical posture. *Exp Brain Res* 235:3449–3457. doi:
34
35 448 10.1007/s00221-017-5069-2
36
37
38
39 449 Colebatch JG, Govender S (2019) Responses to anterior and posterior
40
41 450 perturbations in Parkinson’s disease with early postural instability: role of
42
43 451 axial and limb rigidity. *Exp Brain Res* 237:1853–1867. doi:
44
45 452 <https://doi.org/10.1007/s00221-019-05553-8>
46
47
48
49
50 453 Colebatch JG, Govender S, Dennis DL (2016) Postural responses to anterior and
51
52 454 posterior perturbations applied to the upper trunk of standing human
53
54 455 subjects. *Exp Brain Res* 234:367–376. doi: 10.1007/s00221-015-4442-2
55
56
57
58 456 Diener HC, Horak FB, Nashner LM (1988) Influence of stimulus parameters on
59
60
61
62
63
64
65

- 1
2 457 human postural responses. *J Neurophysiol* 59:1888–1905. doi:
3
4 458 10.1152/jn.1988.59.6.1888
5
6
7
8 459 Dvir Z, Paterna M, Quargnenti M, et al (2020) Linearity and repeatability of
9
10 460 postural responses in relation to peak force and impulse of manually
11
12 461 delivered perturbations : a preliminary study. *Eur J Appl Physiol* 120:1319–
13
14 462 1330. doi: 10.1007/s00421-020-04364-y
15
16
17
18
19 463 Engelhart D, Schouten AC, Aarts RGKM, Van Der Kooij H (2015) Assessment of
20
21 464 Multi-Joint Coordination and Adaptation in Standing Balance : A Novel
22
23 465 Device and System Identification Technique. *IEEE Trans Neural Syst*
24
25 466 *Rehabil Eng* 23:973–982. doi: 10.1109/TNSRE.2014.2372172
26
27
28
29 467 Ferraresi C, De Benedictis C, Muscolo GG, et al (2020a) Development of an
30
31 468 Automatic Perturbator for Dynamic Posturographic Analysis. *Mechanisms*
32
33 469 *ans Machine Science* 93:273–282. doi: 10.1007/978-3-030-58104-6
34
35
36
37
38 470 Ferraresi C, Maffiodo D, Franco W, et al (2020b) Hardware-In-the-Loop
39
40 471 Equipment for the Development of an Automatic Perturbator for Clinical
41
42 472 Evaluation of Human Balance Control. *Appl Sci* 10:8886. doi:
43
44 473 10.3390/app10248886
45
46
47
48
49 474 Forghani A, Preuss R, Milner TE (2017) Effects of amplitude and predictability of
50
51 475 perturbations to the arm on anticipatory and reactionary muscle responses to
52
53 476 maintain balance. *J Electromyogr Kinesiol* 35:30–39. doi:
54
55 477 <http://dx.doi.org/10.1016/j.jelekin.2017.05.006>
56
57
58
59
60
61
62
63
64
65

- 1
2 478 Fujimoto M, Bair WN, Rogers MW (2015) Center of pressure control for balance
3
4
5 479 maintenance during lateral waist-pull perturbations in older adults. J
6
7 480 Biomech 48:963–968. doi: 10.1016/j.jbiomech.2015.02.012
8
9
10 481 Goodworth AD, Peterka RJ (2018) Identifying mechanisms of stance control : A
11
12 482 single stimulus multiple output model-fit approach. J Neurosci Methods
13
14 483 296:44–56. doi: 10.1016/j.jneumeth.2017.12.015
15
16
17
18 484 Grassi L, Rossi S, Studer V, et al (2017) Quantification of postural stability in
19
20 485 minimally disabled multiple sclerosis patients by means of dynamic
21
22 486 posturography: An observational study. J Neuroeng Rehabil 14:4. doi:
23
24 487 10.1186/s12984-016-0216-8
25
26
27
28
29 488 Horak FB, Nashner LM (1986) Central programming of postural movements:
30
31 489 adaptation to altered support-surface configurations. J Neurophysiol
32
33 490 55:1369–81. doi: 10.1152/jn.1986.55.6.1369
34
35
36
37
38 491 Ivanenko Y, Gurfinkel VS (2018) Human postural control. Front Neurosci
39
40 492 12:171. doi: 10.3389/fnins.2018.00171
41
42
43
44 493 Kim J, Kim C, Lee J, et al (2009) Human postural control against external force
45
46 494 perturbation applied to the high-back. Int J Precis Eng Manuf 10:147–151.
47
48 495 doi: 10.1007/s12541-009-0083-3
49
50
51
52 496 Kim S, Atkeson CG, Park S (2012) Perturbation-dependent selection of postural
53
54 497 feedback gain and its scaling. J Biomech 45:1379–1386. doi:
55
56 498 10.1016/j.jbiomech.2012.03.001
57
58
59
60
61
62
63
64
65

- 1
2 499 Maaswinkel E, Griffioen M, Perez RSGM, van Dieën JH (2016) Methods for
3
4 500 assessment of trunk stabilization, A systematic review. *J Electromyogr*
5
6 501 *Kinesiol* 26:18–35. doi: 10.1016/j.jelekin.2015.12.010
7
8
9
10 502 Maffiolo D, Franco W, De Benedictis C, et al (2020) Pneumo-tronic Perturbator
11
12 503 for the Study of Human Postural Responses. *Advances in Intelligent Systems*
13
14 504 and Computing 980:374–383. doi: 10.1007/978-3-030-19648-6_43
15
16
17
18 505 Martinelli AR, Coelho DB, Magalhães FH, et al (2015) Light touch modulates
19
20 506 balance recovery following perturbation: from fast response to stance
21
22 507 restabilization. *Exp Brain Res* 233:1399–1408. doi: 10.1007/s00221-015-
23
24 508 4214-z
25
26
27
28
29 509 Morasso PG, Baratto L, Capra R, Spada G (1999) Internal models in the control
30
31 510 of posture. *Neural Networks* 12:1173–1180. doi: 10.1016/S0893-
32
33 511 6080(99)00058-1
34
35
36
37
38 512 Pacheco Quiñones D, Paterna M, De Benedictis C (2021) Automatic
39
40 513 electromechanical perturbator for postural control analysis based on model
41
42 514 predictive control. *Appl Sci* 11:4090. doi: 10.3390/app11094090
43
44
45
46 515 Pasman EP, McKeown MJ, Cleworth TW, et al (2019) A novel MRI compatible
47
48 516 balance simulator to detect postural instability in parkinson’s disease. *Front*
49
50 517 *Neurol* 10:922. doi: 10.3389/fneur.2019.00922
51
52
53
54 518 Pidcoe PE, Rogers MW (1998) A closed-loop stepper motor waist-pull system for
55
56 519 inducing protective stepping in humans. *J Biomech* 31:377–381. doi:
57
58
59
60
61
62
63
64
65

- 1
2 520 10.1016/S0021-9290(98)00017-7
3
4
5
6 521 Robbins SM, Caplan RM, Aponte DI, St-Onge N (2017) Test-retest reliability of a
7
8 522 balance testing protocol with external perturbations in young healthy adults.
9
10 523 Gait Posture 58:433–439. doi: 10.1016/j.gaitpost.2017.09.007
11
12
13
14 524 Robert T, Vallee P, Tisserand R (2018) Stepping boundary of external force-
15
16 525 controlled perturbations of varying durations : Comparison of experimental
17
18 526 data and model simulations. J Biomech 75:89–95. doi:
19
20 527 10.1016/j.jbiomech.2018.05.010
21
22
23
24 528 Schmidt D, Germano AMC, Milani TL (2015) Aspects of dynamic balance
25
26 529 responses: Inter- and intra-day reliability. PLoS One 10:e0136551. doi:
27
28 530 <http://dx.doi.org/10.1371/journal.pone.0136551>
29
30
31
32
33 531 Shumway-Cook A, Woollacott MH (2007) Motor Control: Translating research
34
35 532 into clinical practice, 3rd edn. Lippincott Williams & Wilkins, Philadelphia,
36
37 533 Pa, USA.
38
39
40
41 534 Sturnieks DL, Menant J, Delbaere K, et al (2013) Force-Controlled Balance
42
43 535 Perturbations Associated with Falls in Older People: A Prospective Cohort
44
45 536 Study. PLoS One 8:e70981. doi: 10.1371/journal.pone.0070981
46
47
48
49 537 Teixeira LA, Azzi N, de Oliveira JÁ, et al (2019) Automatic postural responses
50
51 538 are scaled from the association between online feedback and feedforward
52
53 539 control. Eur J Neurosci 1–10. doi: 10.1111/ejn.14625
54
55
56
57
58 540 Van Der Kooij H, Peterka RJ (2011) Non-linear stimulus-response behavior of the
59
60
61
62
63
64
65

1
2 541 human stance control system is predicted by optimization of a system with
3
4 542 sensory and motor noise. *J Comput Neurosci* 30:759–778. doi:
5
6 543 10.1007/s10827-010-0291-y
7
8
9

10 544 Van Der Kooij H, Van Asseldonk E, Van Der Helm FCT (2005) Comparison of
11
12 545 different methods to identify and quantify balance control. *J Neurosci*
13
14
15 546 *Methods* 145:175–203. doi: 10.1016/j.jneumeth.2005.01.003
16
17

18 547 Winter DA, Patla AE, Prince F, et al (1998) Stiffness control of balance in quiet
19
20
21 548 standing. *J Neurophysiol* 80:1211–1221. doi: 10.1152/jn.1998.80.3.1211
22
23

24
25 549

26
27
28 550

29
30
31 551 **FIGURE LEGENDS**
32

33
34 552 **Figure 1.** Experimental Set-up. A: pneumo-tronic perturbator, 1: low friction
35
36 553 pneumatic actuator, 2: flow-proportional valves, 3: laser sensor, 4: load cell,
37
38 554 5: end striker, 6: handles, 7: trigger button. B: Example of experimental task
39
40
41 555 with the operator handling the pneumo-tronic perturbator.
42
43

44
45 556 **Figure 2.** Force profiles for the different perturbation types included in the constant
46
47 557 force series (A) and the constant impulse series (B). The intended force
48
49 558 profile (red) is superimposed to the actually delivered force profile (blue,
50
51 559 average across all subjects).
52
53

54
55 560 **Figure 3.** A representative recording of the perturbation (Black line) and the
56
57 561 ensuing displacement of the Center of Pressure (dashed grey line) observed
58
59
60

1
2 562 during experimentation (constant-force series: 40 N, 6 Ns).
3
4

5 563 **Figure 4.** Free body diagram of a single-link inverted pendulum model for postural
6
7 564 control analysis. θ is the body oscillation, l is the height of the subject with
8 565 respect to the ankle joint; h_F is the distance between ankle joint and the point
9
10 566 of application of the perturbation force F_e ; d is the distance between ankle
11
12 567 joint and the center of mass (CoM); h is the height of ankle joint with respect
13
14 568 to the fixed base of support; I is the rotational inertia of the body about the
15
16 569 CoM; m is the subject body mass; \ddot{x} is the horizontal acceleration of the CoM;
17
18 570 \ddot{y} is the vertical acceleration of the CoM; $\ddot{\theta}$ is the angular acceleration of the
19
20 571 CoM; g is the gravitational acceleration; τ is the correcting torque at the
21
22 572 ankle; CoP is the center of pressure position; R_x is the horizontal component
23
24 573 of the ground reaction force; R_y is the vertical component of the ground
25
26 574 reaction force
27
28
29
30
31
32
33

34
35 575 **Figure 5.** Characteristics of delivered perturbations for the constant-force series
36
37 576 (left) and the constant-impulse series (right). Each box represents the median
38
39 577 and the standard deviation of the perturbations applied to the subjects (n=5
40
41 578 perturbation x 14 subjects = 70), for each stimulus type.
42
43
44
45

46 579 **Figure 6.** The relationship between the maximum displacement of the center of foot
47
48 580 pressure, ΔCoP , and the magnitude of the perturbations, in terms of impulse
49
50 581 (A) and force amplitude (B) for each participant in the experimental trial.
51
52 582 Distribution of the Pearson's Correlation Coefficients, for the ΔCoP –
53
54 583 Impulse (Black) and the ΔCoP - Force (white) correlation (C).
55
56
57
58
59
60
61
62
63
64
65

1
2 584 **Figure 7.** The relationship between the postural index ΔCoP_n and the magnitude of
3
4
5 585 perturbation expressed in terms of impulse (A) and force amplitude (B) for
6
7 586 each participant in the experimental trial (colored line). The thick black line
8
9 587 represents the average trend.

10
11
12 588 **Figure 8** The relationship between the simulated maximum displacement of the
13
14
15 589 center of foot pressure, ΔCoP , and the magnitude of the perturbations, in
16
17 590 terms of impulse (A) and force amplitude (B). The relationship between the
18
19 591 postural index ΔCoP_n and the magnitude of perturbation expressed in terms
20
21 592 of impulse (C) and force amplitude (D).
22
23 593 Red lines refer to the results of the simulation performed considering the
24
25 594 sensorial noise; blue lines refer to the results of the simulation performed
26
27 595 without the contribution of the sensorial noise; black lines are the average
28
29 596 experimental trend calculated on all the participants of the experimental
30
31 597 analyses.
32
33
34
35
36
37
38
39
40
41
42
43
44
45
46
47
48
49
50
51
52
53
54
55
56
57
58
59
60
61
62
63
64
65

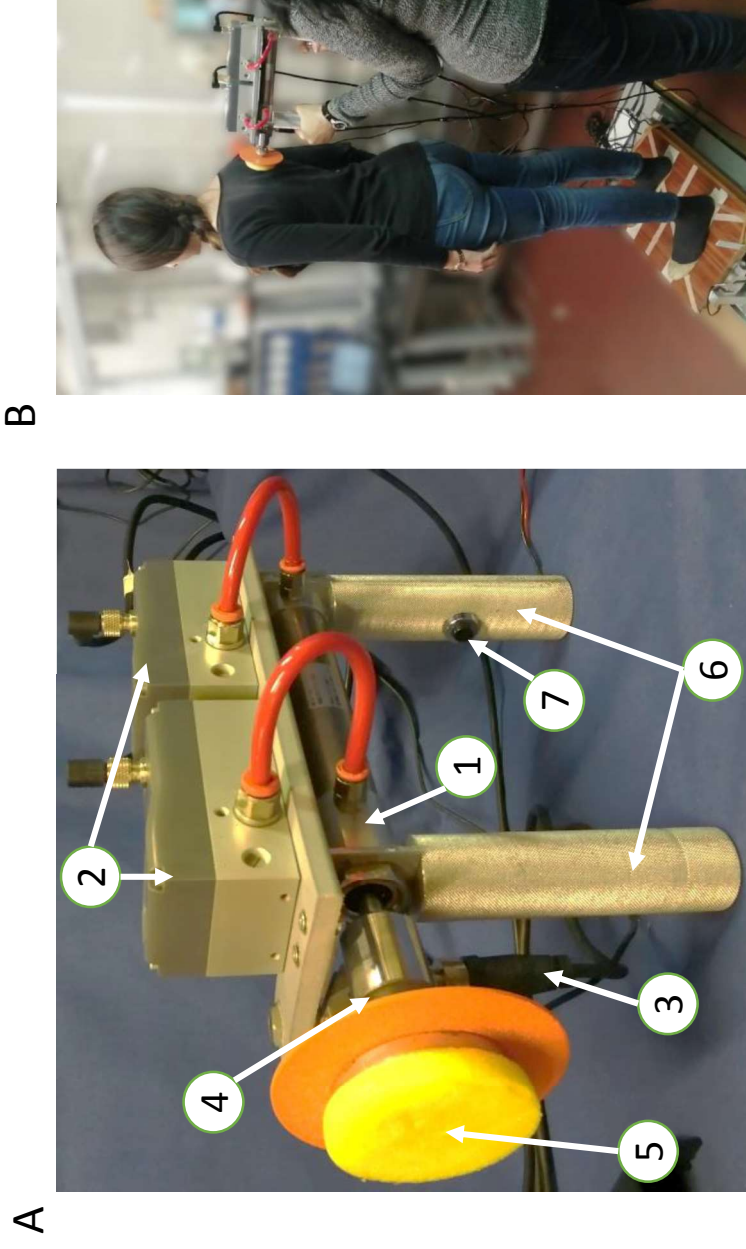


Figure 1

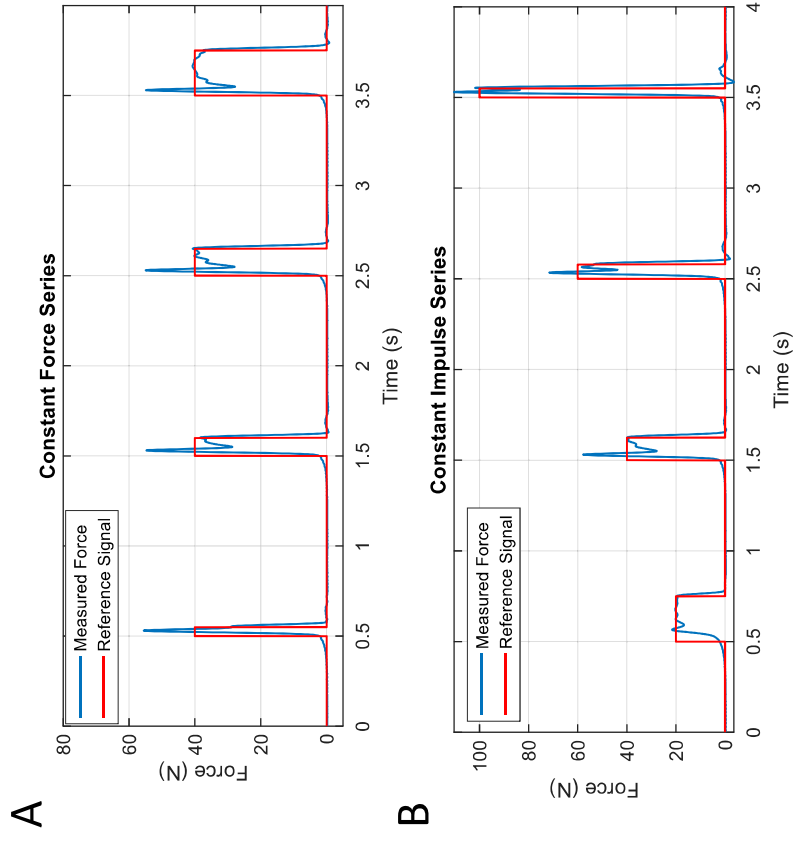


Figure 2

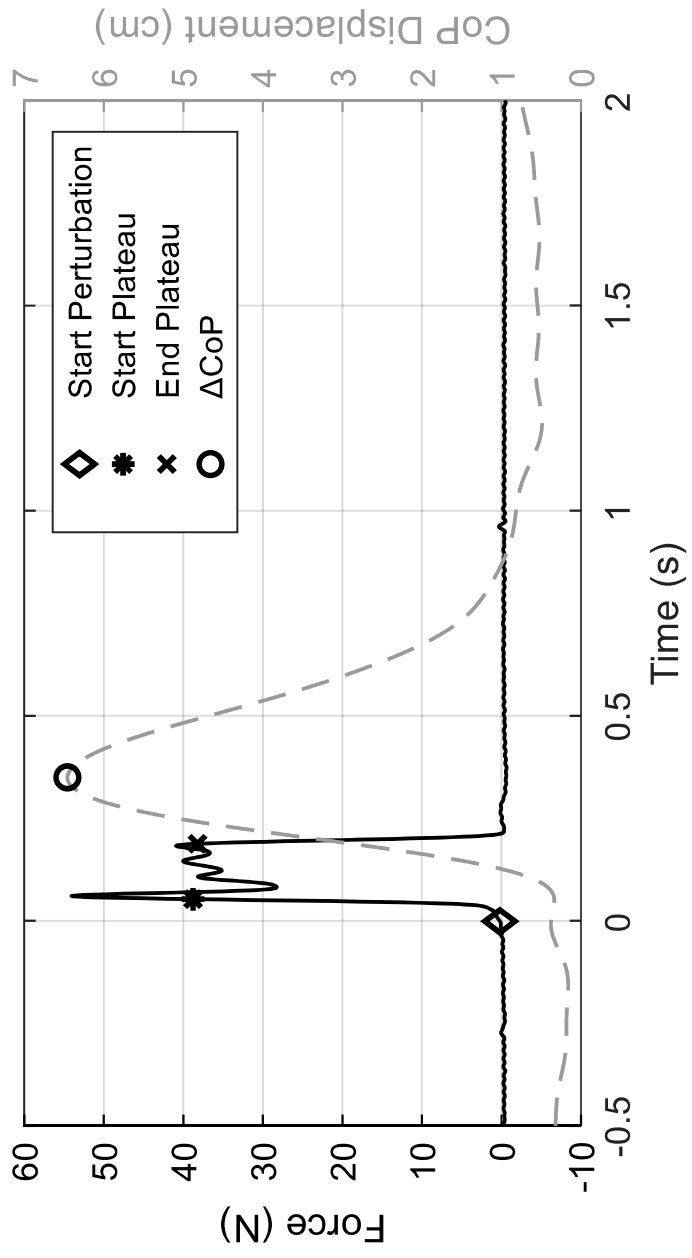


Figure 3

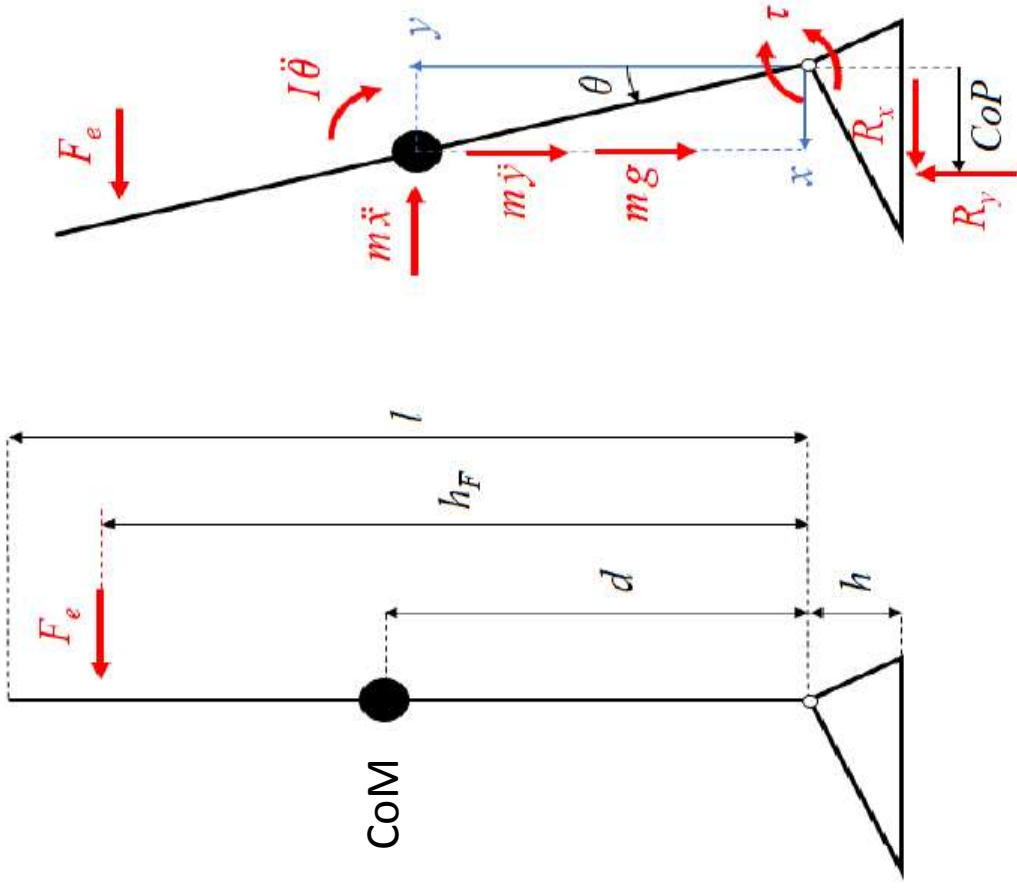


Figure 4

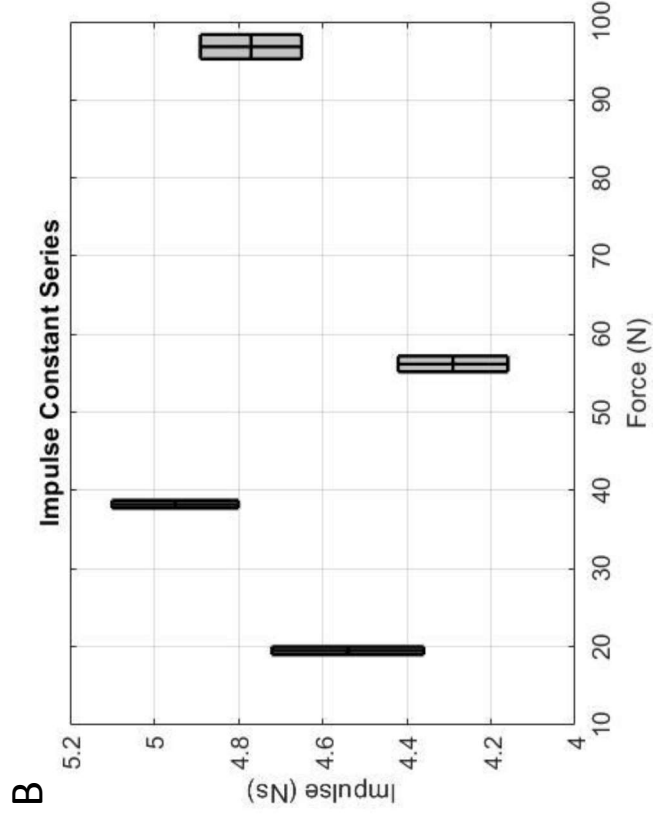
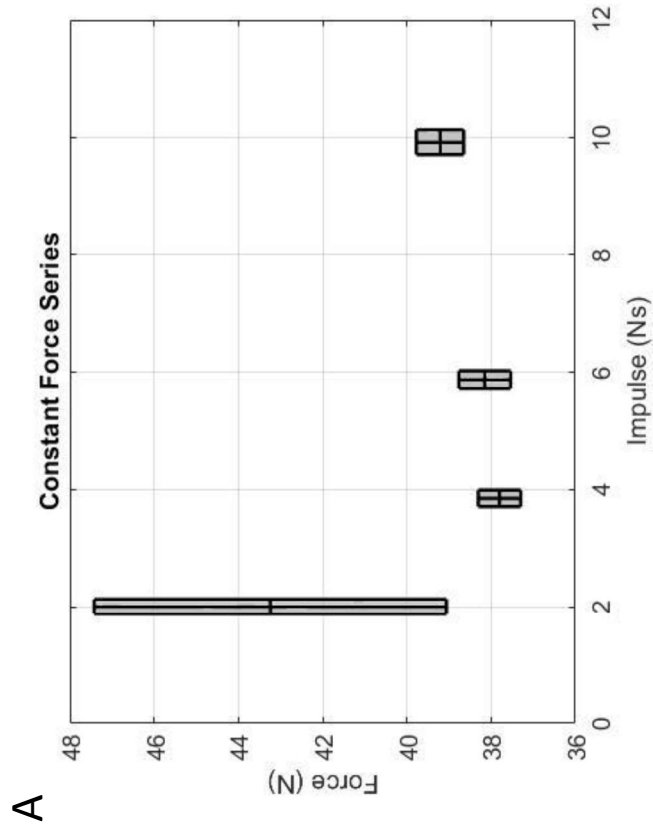


Figure 5

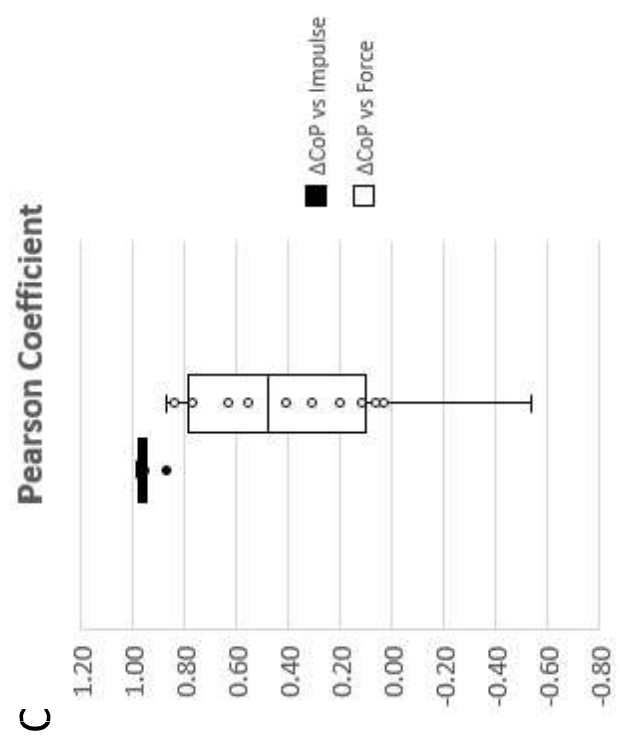
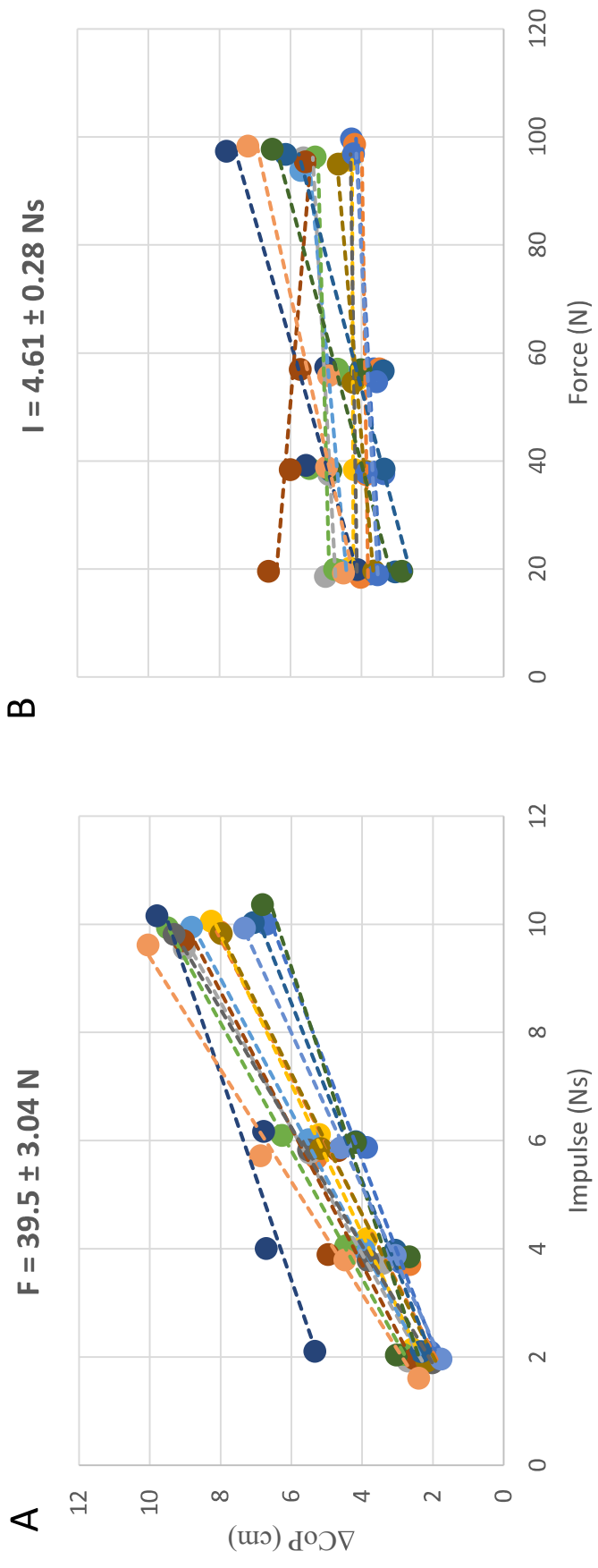


Figure 6

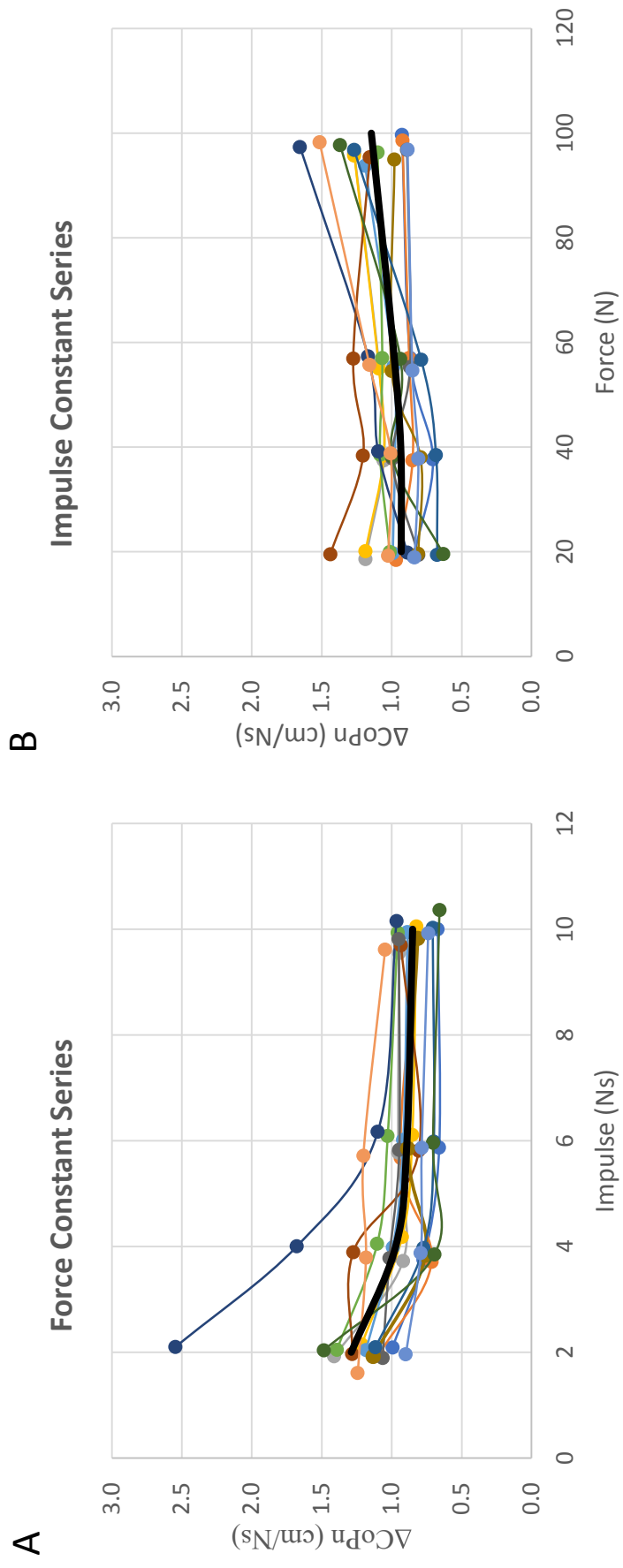


Figure 7

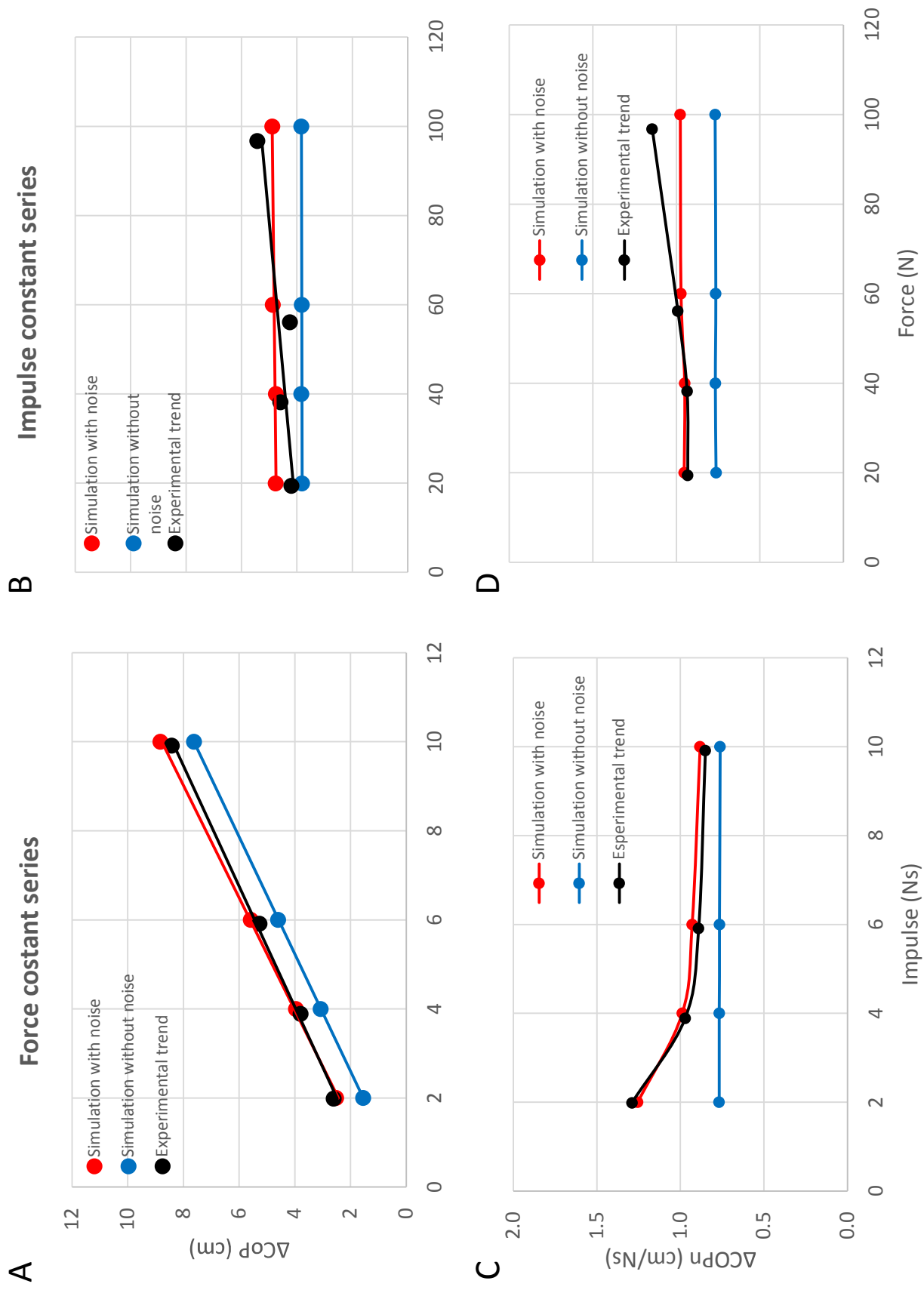


Figure 8